The Journal of Supercritical Fluids 133 (2018) 383–392

Contents lists available at ScienceDirect

The Journal of Supercritical Fluids

journal homepage: www.elsevier.com/locate/supflu

Modification of iPP microcellular foaming behavior by thermal history control and nucleating agent at compressed CO_2

Xiaoli Zhang[a,*], Benwei Li[a], Xihuan Wang[a], Kun Li[a], Gang Wang[a], Jingbo Chen[a,*], Chul B. Park[b]

[a] School of Materials Science and Engineering, Zhengzhou University, Zhengzhou 450001, China
[b] Microcellular Plastics Manufacturing Laboratory, Department of Mechanical and Industrial Engineering, University of Toronto, Toronto, Ontario M5S 3G8, Canada

GRAPHICAL ABSTRACT

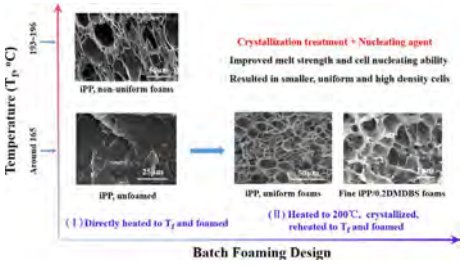

ARTICLE INFO

Keywords:
Isotactic polypropylene
Nucleating agent
Crystallization
Microcellular foaming
Compressed CO_2

ABSTRACT

This study is aimed at using thermal history control and nucleating agent to adjust the foaming behavior of isotactic polypropylene (iPP). Through the introduction of an annealing stage and α nucleating agent, the crystallization and rheological properties of iPP were changed, and its microcellular foaming behavior was tuned correspondingly. Rheological testing results verified the enhancement of melt strength through the presentation of the crystallization stage and α nucleating agent. After an annealing at 110 ˚C, 10 MPa, for 40 min, iPP was further saturated at 165 ˚C, 12 MPa for 30 min and then foamed, the cell density is 7.95×10^9 cells/cm^3, while the average cell size is 11.66 μm. Furthermore, the synergy between the annealing treatment and an addition of 0.2 wt.% α nucleating agent could positively affect the heterogenous cell nucleating ability and melt strength of iPP, much smaller sized cells with relatively quite high cell density up to 10^{13}–10^{14} cells/cm^3 were induced.

1. Introduction

Microcellular foams exhibit unique properties over solid or traditional foamed polymers, such as light weight, material saving, low heat conductivity, and high impact strength, these advantages enable microcellular foams to be received significant attentions in the past several decades [1–4]. Compressed CO_2 is usually used in microcellular foaming process, as a physical foaming agent, primarily because it is inexpensive and safe in performance [4]. Compared with other microcellular foamed polyolefin materials such as polystyrene (PS) or polyethylene (PE), Polypropylene (PP) foams have higher service temperature, rigidity and thermal stability. Additionally, PP foams offer a good impact strength than PS foams, and a higher strength than PE foams [5,6]. PP foams are the promising substitutes for other polyolefin thermoplastic foams in various industrial applications. Being one of universal synthetic polymer materials, iPP has been popularly applied in packaging, household appliances, heat insulating, automobile parts, and other industrial fields. However, iPP is difficult to be foamed to a fine cell morphology level. The main reason is ascribed to its liner molecular structure, which results in a too low melt strength and

* Corresponding authors.
E-mail addresses: zhangxl@zzu.edu.cn (X. Zhang), chenjb@zzu.edu.cn (J. Chen).

https://doi.org/10.1016/j.supflu.2017.11.003
Received 3 September 2017; Received in revised form 5 November 2017; Accepted 6 November 2017
Available online 07 November 2017
0896-8446/

hinders the generation of ideal cell morphology. Cell collapse, coalescence or rupture developed during melt foaming are the severe defects of iPP microcellular foams [5].

To improve iPP's melt strength, some methods were adopted, for instance, grafting, blending of liner or branched polymers, and filling of additives are the prevalent approaches had been used. Introducing of the functional end groups or blending a long chain branched structure into the PP backbone molecule is an effective way to enhance its foamability [7–10]. Zhai et al. [7] reported that the branched or grafted iPP revealed well-defined close cell structure and increased cell density resulted from increased melt strength, compared to that of liner iPP. According to other literatures, blending with another polymer was extensively used to adjust the PP cell structure and its foaming behavior [11–14]. Huang et al. [12] and Rachatanapun et al. [13,14] investigated the influences of HDPE and PS on the PP foaming properties, respectively. Zhang et al. [15] cooperated PP/HDPE blends with dynamic shear action, they found that the enhanced melt strength could effectively restrict cell growth, improve the foamability, and prevent the cell rupture. Moreover, other additives such as nanoclay [16], calcium carbonate particle [1,17–19], crystal nucleating agent [20], and natural fiber [21–24] were utilized to reinforce the PP foams. Even the above mentioned methods could increase the foamability of iPP, but those treatments might increase the cost obviously, or deteriorate some mechanical properties of the final foamed products.

It is well known that iPP is a typical semi-crystallized polymer material, it has a fast crystallization rate and presents relatively higher melting temperature point, compared to PE or PS, the microstructure transformation of iPP during processing will affect the final product property. For microcellular foaming, recent researches reveal that crystal could play as the so-called heterogeneous cell nucleating effect to assist producing cells with higher density as well as smaller size [25–28]. Crystallization plays an important effect on microcellular foaming process of semi-crystalline polymer materials. Generally, crystals act as a pair of ambivalent functions for iPP foaming, on one hand, a suitable content of crystal may increase the melt strength and produce more cell nucleating sites, which will obviously increase the cell density. On the other hand, too high crystallinity means low saturation volume and difficult diffusing of the foaming agent, which will suppress the iPP expansion. Former researches revealed that physical foaming agent usually could not dissolve in crystal domain, but could easily saturate in amorphous region [25,27,29–33]. To investigate the influence of the crystals on iPP microcellular foaming characteristics, some experiments were developed. Li et al. [27] studied the iPP foaming behavior after erasing the crystallization history, a result of broadening the foaming temperatures from 4 to 40 °C was reported. Jiang et al. [26] investigated the impact of spherulite structure on the cell morphology of iPP solid-state made foams, and the generation of microcells in the amorphous regions located in the interlamellar and boundaries of iPP spherulites was observed.

In previous batch foaming studies, the semi-crystallized polymer materials with a low crystallinity could absorb much more pressurized physical foaming agent at a solid state, compared to that of a high crystallized counterpart. Baldwin et al. [34,35] investigated the foaming differences between amorphous and semi-crystallized PET, the crystallized PET samples with a crystallinity of about 10% have higher cell densities than that of amorphous ones. Doroudiani et al. [36] fabricated semi-crystallized HDPE, PB, PP and PET with different crystallinities obtained through different cooling rates. The foaming results indicated that more uniform cells were derived from the samples with a lower degree of crystallinity, but the non-uniform or unfoamed structures were made in the samples at a higher crystallinity level, the latter one was originated from a slow cooling rate. Zhai et al. [37] studied the improved crystallization behavior of PLA at a compressed CO_2, and its effect on the foaming property of PLA. Usually, the precondition of higher blowing agent sorption in a semi-crystallized solid polymer is its comparatively lower original degree of crystallinity, because the blowing agent can only easily dissolve in the amorphous phase. But for the received iPP pellet in this study, its virgin crystallinity is as high as 54.11%, which means a rather low CO_2 absorption ability at a solid phase. In order to improve the solubility of supercritical CO_2 in iPP and its foaming morphology, iPP should be firstly melted, and then be foamed at a relatively high temperature [26] or below its melting point [27,33], the melt strength is less strong in those circumstances to withstand the blowing elongation forces, which will affect its foaming morphology and structure.

Based on the understanding of the effect of partially melted iPP on its crystallization properties [38–42], we first tried to modulate the melt strength and microcellular cell nucleating ability of iPP through its melt self-enhancement via a thermal history control. Moreover, the influence of a low loading content of 0.2 wt.% DMDBS (Bis (3, 4- dimethylbenzylidene) sorbitol) nucleating agent on fabricating fine iPP foams, cooperated with the above mentioned thermal history design was also investigated in this paper.

2. Experimentation

2.1. Materials and sample preparation

A semi-crystalline iPP (Ningxia China, Brand No. T30S) was used in this experiment. It has a specific gravity of 0.90–0.91g/cm^3, isotactic degree ≥ 95.0%, and the melt index of 3.5 g/10 min (at 210 °C, 2.16 kg). A α type nucleating agent DMDBS of Miiiad 3988 (powder shape) was selected as an additive, which was produced by Milliken company in America. Carbon dioxide (CO_2) (99.5% purity, supplied by Zhengzhou Qiangyuan chemical company, China) was used as a physical foaming agent.

IPP pellets were compressed into thin samples with a thickness of 1.5 mm, length of 50 mm and width of 10 mm, using a laboratory model presser, typed of FM450, made by Beijing Fuyouma technology company, at 200 °C, 6 MPa for 10 min (5 min for melting, and 5 min for holding). The nucleating agent 0.2 wt.% DMDBS added sample was compounded by a twin screw extruder (JIEENTE company, Nanjing, China) before compression, the L/D of the screw is 40, and the screw diameter is 20 mm. The screw speed was set as 80 r/min, five zone temperatures from 175 to 230 °C at the feed hopper to the die were arranged. The compounded pellets were further compressed into discs or thin plates and prepared for rheological testing or batch foaming, respectively. The compressed plates were cut to 10 × 10 mm (length × width) sized samples for further batch foaming using the assembly equipment shown in Fig. 1.

For rheological testing, the thickness of 1.0 mm iPP and 0.2 wt.% DMDBS added iPP discs with the diameters of 25 mm were compressed using the same presser and conditions mentioned above. To ensure the reliability and repeatability of the results, each rheological experiment was conducted for at least three times.

2.2. Rheological characterization

To understand and verify the impact of the crystallization or annealing treatment and nucleating agent on iPP's rheological property, the experiments were performed with a rheometer (ARES-G2, TA Instruments) using parallel plate fixtures at a gap of 1.5 mm, fixed strain of 0.1%, frequency of 1.0 Hz, in the oscillatory mode.

As shown in Fig. 2, all samples were firstly heated to 210 °C and held for 5 min to erase the former thermal and mechanical histories, one pure iPP sample (marked as iPP-NC, without the crystallization treatment) was cooled to 165 °C, which is next to iPP's melting temperature, at a cooling rate of 10 °C/min. When the temperature reached and stabilized at 165 °C, a duration of 15 min was applied and the storage modules (G'), loss modules (G”), and complex viscosity (η*) were measured under the time sweep at a given strain of 0.1%. Another pure iPP (marked as iPP-C, with the crystallization treatment) and 0.2%

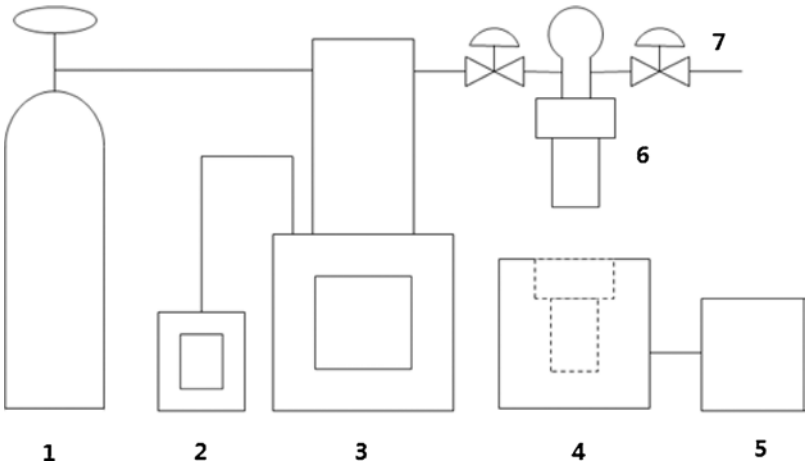

Fig. 1. Home-made batch foaming equipment.
1-Gas cylinder 2-Gas pump controller 3-Gas pump 4-Thermoregulation apparatus 5-Thermoregulation apparatus controller 6-High-pressure vessel 7-Valve.

nucleating agent added iPP (marked as iPP/0.2DMDBS-C) were cooled to 130 °C after a holding time of 5 min at 210 °C, crystallized at 130 °C for 15 min, after that, the samples were reheated to 165 °C, for another holding time of 15 min, and the related data were recorded simultaneously.

2.3. Batch foaming process

Batch foaming experiments were conducted in a high-pressure vessel, which is a part of home-made batch foaming equipment shown in Fig. 1, temperatures were controlled by the home-made precise electrical heating apparatus and the related controllers. The vessel was heated to 200 °C and stabilized for 10 min. Low pressurized CO_2 was used to purge it for three times, furthermore, the compressed CO_2 was charged to a pressure required value.

To contrast the influence of the partially melted iPP on its foamability, iPP foams were also fabricated at a high temperature of 193 °C, which was directly heated from room temperature. And another series of samples were made at 165 °C, after eliminating of previous thermal history at 200 °C.

For the foaming introduced with an annealing or crystallization stage, a batch foaming process was conducted as shown in Fig. 3. Samples were firstly heated to 200 °C and held for 20 min to eliminate the original thermal and mechanical histories, as well as allowed them to saturate the pressurized CO_2 as much as possible (stage 1 in Fig. 3). Secondly, the samples were cooled to different annealing temperatures (T_a of 100–140 °C, with a 10 °C interval, P_a of 10 MPa) for 40 min isothermal crystallization (a suitable T_a of 110 °C was chosen for further foaming through a trial and error process, (stage 2 in Fig. 3)). Finally, the samples were reheated to a higher temperature (T_f), for a duration of 30 min (stage 3 in Fig. 3), pressures were rapidly released and the vessel (with sample) was immediately dipped into a cold water bath to freeze and stabilize the cell structure.

2.4. Differential scanning calorimetry (DSC) analysis

Differential Scanning Calorimeter (NETZSCH 204, Germany) was used to investigate the thermal properties of the neat iPP and iPP/0.2DMDBS foams. The sample was heated at a rate of 10 °C/min to record the heat flow from 25 to 210 °C, Nitrogen was used to protect the samples from degradation. The crystallinity was calculated using the following Eq. (1).

$$X_{DSC} = \frac{\Delta H_i}{\Delta H_i^0} \quad (1)$$

where X_{DSC}: Crystallinity of the sample. ΔH_i^0: Theoretical heat of fusion for 100% crystalline iPP, which is 209.0 J/g [27].

2.5. Scanning electron microscopy (SEM)

The cell morphologies of neat iPP and iPP/0.2DMDBS foams were investigated using a scanning electron microscope (SEM) (JSM-7001F, JEOL, Japan). Foams were fractured after immersion into liquid nitrogen for about 30 min. The fractured surfaces were golden-coated

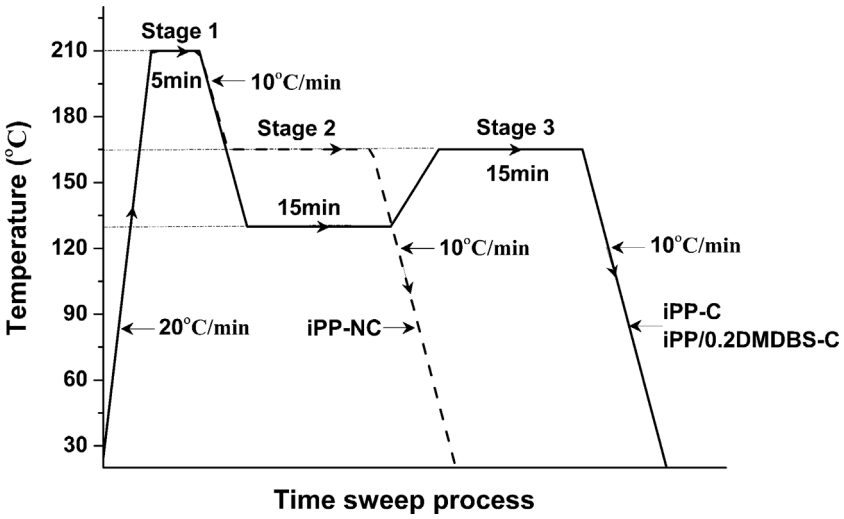

Fig. 2. Schematic of rheological testing design.

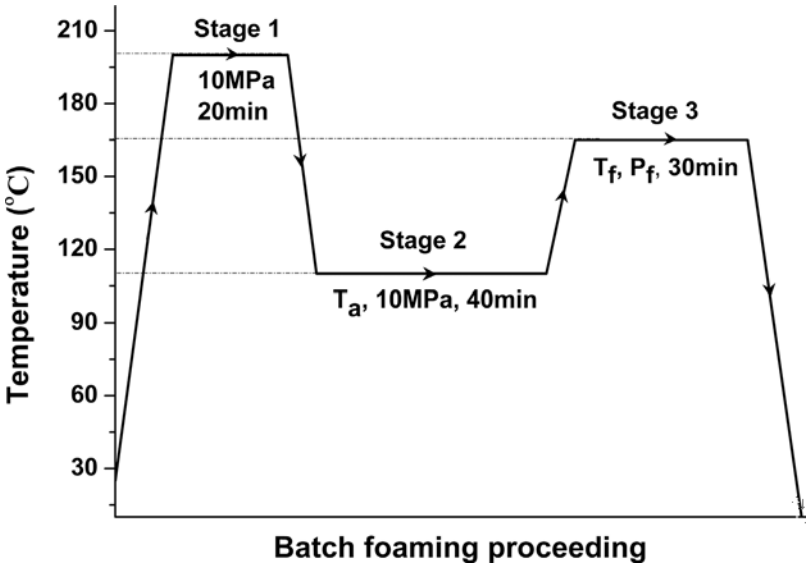

Fig. 3. Schematic of batch foaming procedure design.

before the SEM testing. The foams' expansion ratio was calculated as follows using Eq. (2):

$$\Phi = \frac{\rho_{\text{unfoam}}}{\rho_{\text{foam}}} \tag{2}$$

where ρ_{unfoam} and ρ_{foam} are the densities of the composites before and after foaming, respectively. Both foams were measured according to the ASTM D792 standard using the water displacement method.

The cell size was measured and calculated from the SEM micrographs, and the cell density N was obtained from Eq. (3) as follows [7]:

$$N = \left(\frac{nM^2}{A}\right)^{3/2} \Phi \tag{3}$$

where n is the number of cells counted in the SEM micrograph, M is the magnification factor, A is the analyzed area in cm^2 of the counted area, and Φ is the sample expansion ratio. Image-J software was used to calculate the cell parameters [43].

3. Results and discussion

3.1. Rheological testing

To study the influence of thermal history with or without a crystallization stage on the rheological properties of iPP at a scanning temperature of 165 °C near to its melting point, the experiments illustrated in Fig. 2 were performed. Fig. 4a–c shows the storage module G', loss module G", and complex viscosity η* of the iPP samples, as a function of holding time. We can clearly observe that G', G" and η* of iPP-Cs, which were treated with a duration of 15 min at a lower temperature of 130 °C, gradually increased with the elongation of the testing time, compared with that of iPP-NC (no crystallization treatment). At the testing temperature, the existence of partially ordered iPP melt structure, originated from the crystallization stage [38,44], might serve as the key enhancement factor on the melt strength [38], and the structured melt might easily crystallize and finally influence iPP's foamability, because of its self-nucleation effect [45]. The absolute values (G', G" and η*) of iPP-C are all higher than that of iPP-NC, and iPP-C reveals a time hardening phenomenon, due to the gradually intensified chain entanglement [38]. This increase means the reinforcement of the melt strength of iPP after an introduction of an isothermal crystallization from stage 2 in Fig. 2, and which might work on microcellular foamability enhancement of iPP [46,47]. Moreover, iPP-NC presents almost to a straight line, because it was directly cooled from 210 °C without any existence of original melt structure at the testing temperature [39]. The influence of melt memory effect or the so-called self-nucleating on the polymer crystallization have been extensively reported [38,48]. Zhu et al. [38] studied the accelerating result of partially melted iPP on its nucleating sites and the linear growth rate of spherulite. Tan et al. [48] investigated the speeding effect of metastable melt on the crystallization behavior of poly(ether ether ketone)(PEEK). The metastable melt recrystallized immediately and induced new thicker lamellae among the existing main lamellae, only if there is enough time for the chains to reorganize. Rheological inspection in this study validated the above mentioned experimental phenomenon and the enhancement of the partially ordered melt structure on iPP's rheological property.

Added with a 0.2 wt.% loading nucleating agent, the positive effect of the crystallization influence on the rheological property of iPP is obviously strengthened, as reveled in Fig. 4a. At the end of 15 min holding time at 165 °C, G' of iPP/0.2DMDBS-C reached to 140,330 Pa, compared to that of 17,700 Pa of iPP-NC, the similar η* change occurred between iPP/0.2DMDBS-C and iPP-NC. At 130 °C, the filling of DMDBS increased nucleating sites of crystalline, decreased the crystal size [20]. When the samples were heated to 165 °C, crystals were partially melted [38,44]. With the prolonging of scanning time, the so-called segmentally ordered melt or structured melt gradually aggrandized the melt strength through the chain folding. Additionally, tanδ = G"/G' indicates the changing tendency between storage and loss modules. Fig. 4d illustrates that the crystallization treated history could affect tanδ of iPP, clearly, the increases of storage modules of crystallized samples are faster than that of loss modules, and the enhancement of storage modules can benefit the elongational endurance of the cell growth.

3.2. Batch foaming experiments

3.2.1. Foaming without a crystallization treatment

According to former studies, iPP has a narrow temperature foaming window in the batch foaming process [26,27,29]. For contrasting with the introduction of the crystallization (or annealing) treatment, a series experiments were performed to figure out their differences in foaming ability. Pure iPP samples were directly heated to a temperature higher than its melting point (e.g. 170–200 °C, with a 10 °C interval), for 2hr duration. At this circumstance, relatively uniform foams were only obtained at 193–196 °C. Fig. 5 presents SEM pictures of iPP foams made at 193 °C, but different pressures of 13, 15 and 18 MPa. Values of average cell sizes and cell densities are listed in Table 1. The results are

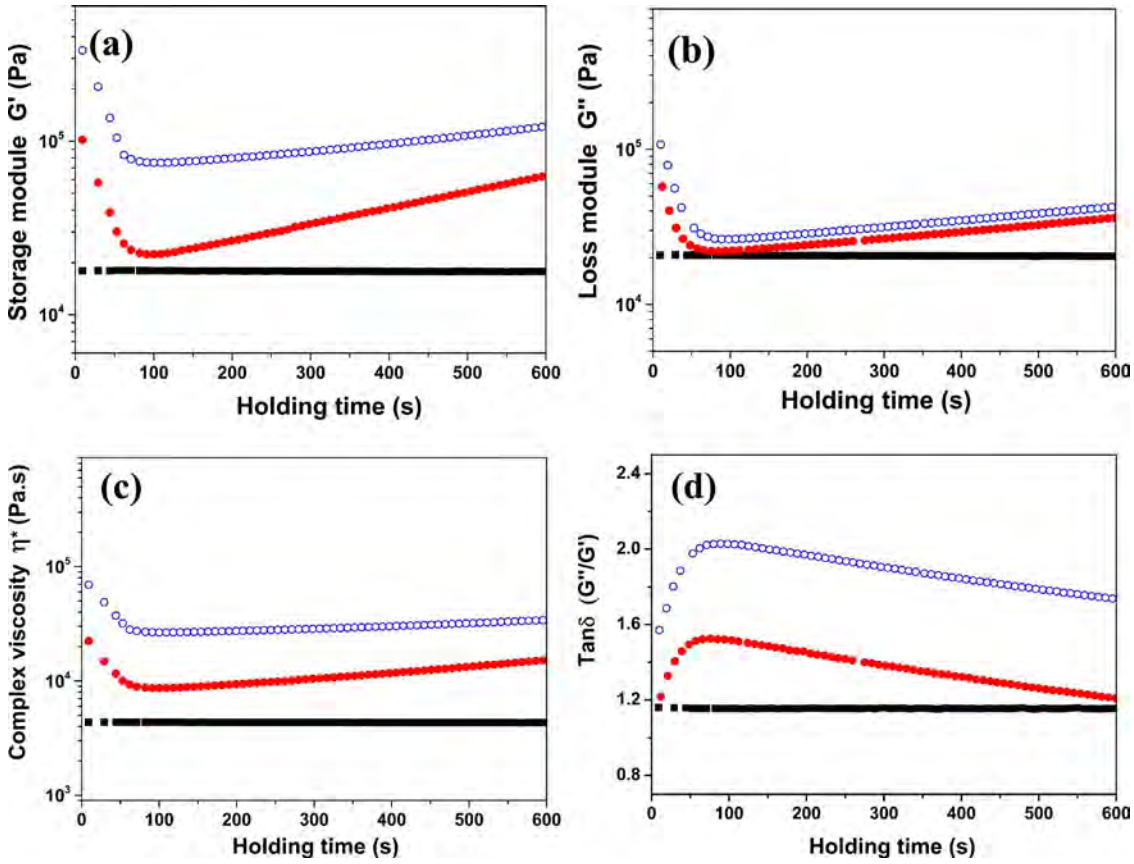

Fig. 4. (a) Storage modules, G', (b) Loss modules, G", (c) Complex viscosities, η*, (d) Tan δ, as a function of holding time at 165 °C, ■ represents iPP-NC (Pure iPP without crystallization treatment), ● represents iPP-C (Pure iPP with crystallization treatment), ○ represents iPP/0.2DMDBS-C (iPP/0.2DMDBS with crystallization treatment).

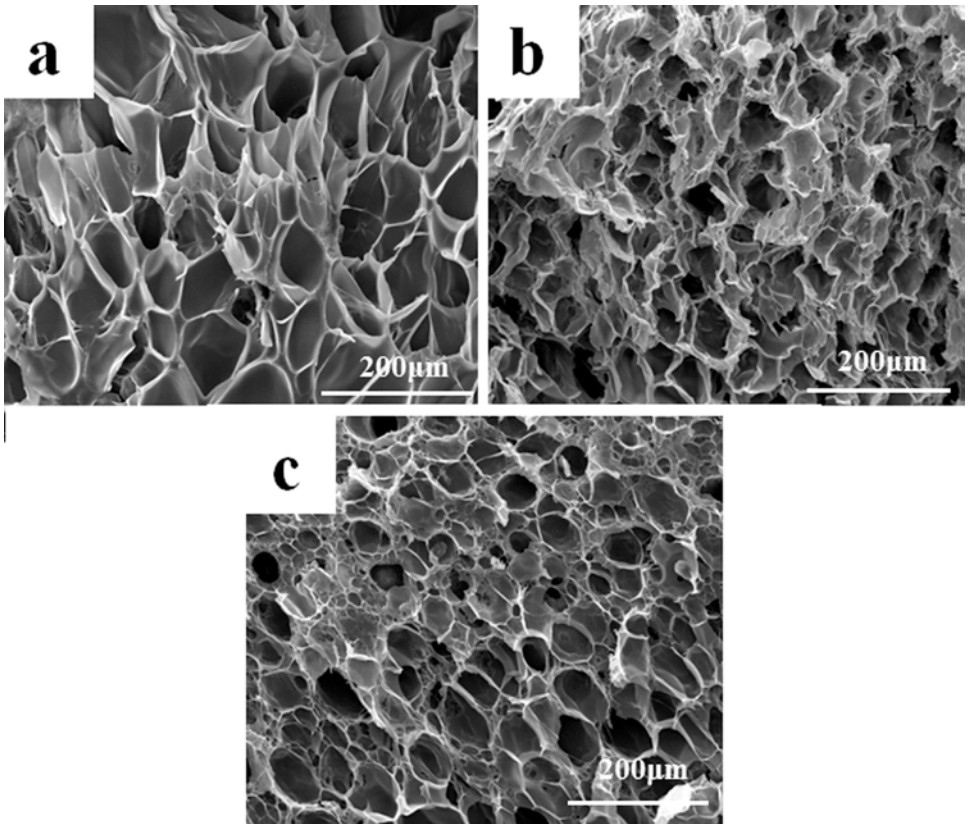

Fig. 5. SEM pictures of foamed iPP at 193 °C, but different P_f of (a) 13 MPa, (b) 15 MPa, (c) 18 MPa.

Table 1
Average cell sizes, cell densities and foam densities of iPP foamed at 193 °C, but different Pf.

P_f (MPa)	13	15	18
Cell size (μm)	36.95	38.61	20.97
Cell density (cells/cm^3)	3.85×10^7	3.32×10^7	2.07×10^8
Foam density (g/cm^3)	0.51	0.50	0.13

similar to the literatures reported [26], as discussed above, at the foaming temperature, melt strength is low, cell wall thickness is thin (Fig. 5a), and the cell morphology is not very uniform (Figs. 5b and 5c). With the increasing of P_f, foam densities decrease from 0.51, 0.50 to 0.13 g/cm^3.

For another case, after eliminating any former thermal history at 200 °C (10 MPa, 20 min), the samples were directly decreased to the temperature of 165 °C (10 MPa), after a holding time of 40 or 80 min, the samples were prepared. From Fig. 6a and b, we can find that the specimens could almost not be foamed, due to the too low melt strength to hold the compressed CO_2 while the depressurizing was exerted. This result agrees with the reported foaming temperature window information [27].

3.2.2. Foaming at 165 °C but different foaming pressures, after a crystallization treatment

As illustrated in the rheological testing, crystallization history and the introduction of partially ordered melt structure could increase the storage modulus obviously at a semi-melting state (165 °C in this study). A step thermal control procedure was introduced to subject iPP samples to a crystallization history, as illustrated in Fig. 3 during stage 2. The selection of crystallized temperature is important in this batch foaming design, because of the plasticizing effect of pressurized CO_2, the glass transition temperature, the melt point, and crystallization temperature will all move to the lower temperatures side [27,37]. Li et al. [27] figured out a T_c changing map of iPP related to CO_2 pressure and cooling rate using a high pressure DSC measurement, which indicated that a T_c of 110 °C induced at 10 MPa and 5 °C/min cooling rate. In this study, a series of foaming experiments were conducted at a given pressure of 10 MPa, but different temperatures from 100 to 140 °C, with a 10 °C interval, and the samples were further foamed at 165 °C, P_f of 12 MPa. Because the annealing temperatures of 130 and 140 °C are too high for iPP to crystallize at 10 MPa, due to the plasticization effect [27], so samples treated at those two temperatures could almost not be expanded. Under 100, 110 and 120 °C annealing temperatures, samples were foamed, but the cell morphology of 110 °C case is more uniform then the others, and the cell density is around $\sim 10^9$ cells/cm^3, compared to $\sim 10^7$ cells/cm^3 of that treated at 100 and 120 °C. From these exploring experiments, we can find that after a 110 °C annealing treatment, the cell sizes become small, and the cell densities clearly excel that reported in the literatures of foamed iPP. Because of the plasticization effect under the compressed CO_2, the iPP crystallization temperature decreased to a lower point than that at ambient pressure. From the literatures, at 10 Mpa CO_2 pressure, the iPP crystallization peak was lowered to about 110 °C [27,29,46], a duration time of 40 min was supposed to enough long for the formation of crystals at this annealing temperature. So 110 °C was selected as the crystallization temperature for further foaming experiments.

To better understand the effect of partially ordered melt and annealing treatment conditions on iPP's foaming behavior, samples were prepared at a fixed T_a of 110 °C, P_a of 10 MPa, but different P_f of 10, 12, 14, and 16 MPa, and a same T_f of 165 °C. SEM pictures of the cell morphologies are presented in Fig. 7. Fig. 7a shows the thicker wall but non-uniform cell structures, because the foaming pressure is relatively low, during the crystallization process, the former dissolved CO_2 was propelled for the reason of solidification. Furthermore, in the duration period before foaming, the CO_2 solubility was limited compared with that at higher pressure counterparts. On the country, too high pressure of 16 MPa, means the increased CO_2 solubility, but at the same time, the plasticization effect directly moved the melting point to a lower temperature point, which aroused the weakening of melt strength, so the wall thickness was thinned and cell coalescence happened in Fig. 7d. Fig. 7b and c is the fractured foams interfaces at the medium pressures of 12 and 14 MPa, smaller sized and uniform cells indicate the improved cell morphologies in these two cases. This is individually approved by the statistic values of average cell sizes and cell densities in Table 2. Clearly, the overall cell sizes decreased, and the cell morphology is improved, while the higher cell densities of 7.30×10^9, 7.95×10^9 cells/cm^3 were formed at P_f of 12 and 14 MPa, respectively. Foam densities in Table 2 decrease from 0.59, 0.31, 0.17 to 0.13 g/cm^3, according to the P_f increasing sequence.

Fig. 8 records the DSC heating traces of the foamed iPP illustrated in Fig. 7. A typical α crystal melting peak appears in around 170 °C, which is about 10 °C higher than 164.4 °C of original received iPP pellets, due to the crystallization, annealing, and recrystallization during the progress of foaming strategy, more stable crystals were generated. These compact packed crystalline lamellars served as the so-called heterogeneous nucleating cell sites in the foaming process. The shoulder peaks left to the melting summits can be identified in the DSC graphs, which usually are explained as the less perfect or incompact lamellars [49–51]. To our knowledge, these less packed crystals might be formed by the rapid temperature jump through the depressurization and elongational stress during the cell developing procedure. It is not clear yet whether these imperfect crystals can generate new cell nucleating sites or not. Moreover, with the increase of P_f, the enthalpy corresponded to the high melting point gradually decrease, which hints the depression of increased pressurized CO_2 on the generation of perfect crystals [52].

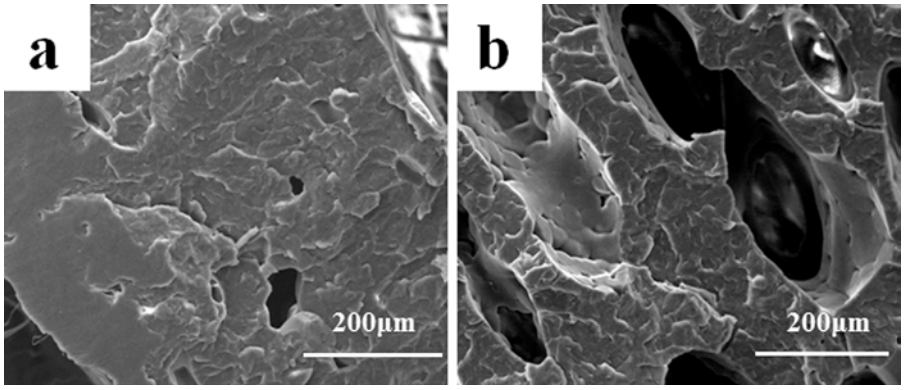

Fig. 6. SEM pictures of foamed iPP at 165 °C, but different saturation time of (a) 40 min, (b) 80 min without a crystallized stage.

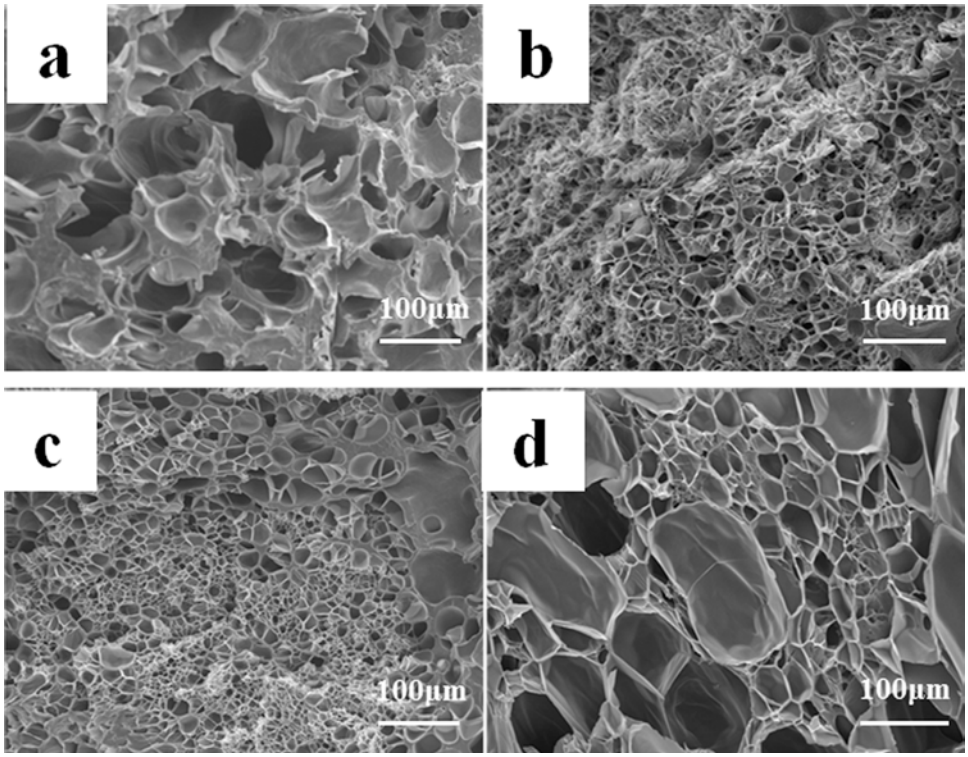

Fig. 7. SEM pictures of foamed iPP, at a fixed foaming temperature of 165 °C, but different pressures of (a) 10 MPa, (b) 12 MPa, (c) 14 MPa, (d) 16 MPa.

Table 2
Average cell sizes, cell densities, and foam densities of iPP foamed at 165 °C, but different Pf, after a crystallization stage treatment.

P_f (MPa)	10	12	14	16
Cell size (μm)	45.90	10.08	11.66	54.61
Cell density (cells/cm^3)	5.35×10^7	7.30×10^9	7.95×10^9	5.89×10^7
Foam density (g/cm^3)	0.59	0.31	0.17	0.13

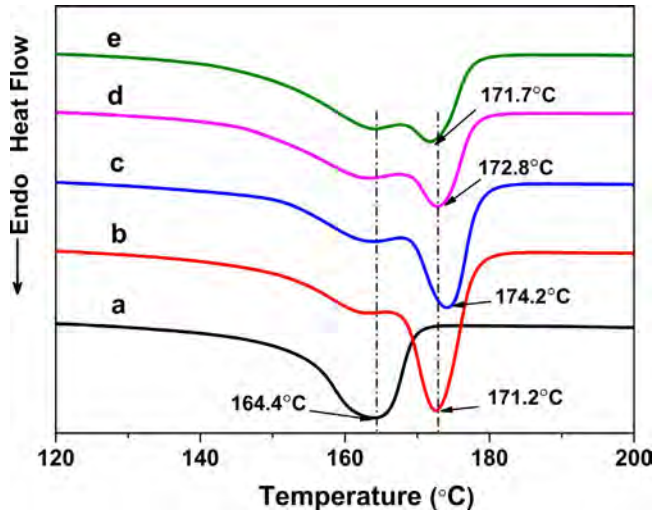

Fig. 8. DSC graphs of unfoamed pure iPP pellets (graph a), and foamed iPP (graphs b–e) at a fixed foaming temperature of 165 °C, but different P_f of a at ambient pressure, b at 10 MPa, c at 12 MPa, d at 14 MPa, and e at 16 MPa.

3.2.3. Foaming with a crystallization treatment and cooperating with a nucleating agent addition

Nucleating agent is usually used to accelerate the crystallization course of the polymers. In this study, a α type nucleating agent of DMDBS was used to modify the crystallization and foamability of iPP. DMDBS not only acts as the normal function of nucleating agent, but also plays as a heterogeneous cell nucleating agent in this study. In order to fabricate smaller cells, except for applying the same step thermal control process as illustrated in section 3.2.2, a 0.2 wt.% content of DMDBS was introduced. The treatment and foaming conditions used here are the same as indicated in Fig. 7.

Fig. 9 shows the SEM pictures of the foamed iPP/0.2DMDBS at different P_f. Generally, because of the robust nucleating effect and the improvement in melt strength, cells with fine shape and morphology were obtained, compared to that of pure iPP at the same foaming condition, this fact further verifies the reinforcement of the melt strength cooperated with DMDBS, which is already discussed in the rheological testing result. The addition of DMDBS increased the number of crystal nucleating sites, and resulted in the improvement of iPP melt elongation property, relatively uniform, small sized fine cells with rather high cell densities were produced, as illustrated in Table 3. The cell densities of about 10^{13}–10^{14}cells/cm^3 were generated, which are predominant to about ~10^7 or ~10^8 cells/cm^3 reported in the literatures [27,29,33]. Foam densities of iPP/0.2DMDBS at different P_f decrease from 0.50 to 0.26 g/cm^3, which are higher than that of pure iPP foams (in Table 2) at the same P_f foaming condition.

DSC testing results of the foamed iPP/0.2DMDBS as shown in Fig. 9 are presented in Fig. 10, after filling with the nucleating agent, the crystallinity increased slightly, compared to that of pure iPP foams. With the increase of foaming pressure P_f, the crystallinity slightly decreased, from 53.4, 50.1, 42.9 to 41.8%, corresponding to the P_f of 10, 12, 14, and 16 MPa, respectively. The appearance of DMDBS moved the melting point to the lower temperature, compared with the pure iPP foams (see Fig. 8). The addition of DMDBS might increase the crystal nucleating sites, rather than accelerate the crystal growth, so numerous small sized crystals generated and hindered the prefect stacking of the lamellars [20,53]. Meanwhile, the shoulder peaks were also generated in the nucleating agent added samples, which indicate the emergence of imperfect crystals.

Microcellular batch foaming behavior is usually sensitive to the saturation temperature and pressure. To fabricate much small cells, a lower T_f of 162 °C, P_f of 10 MPa were set, other parameters used are as

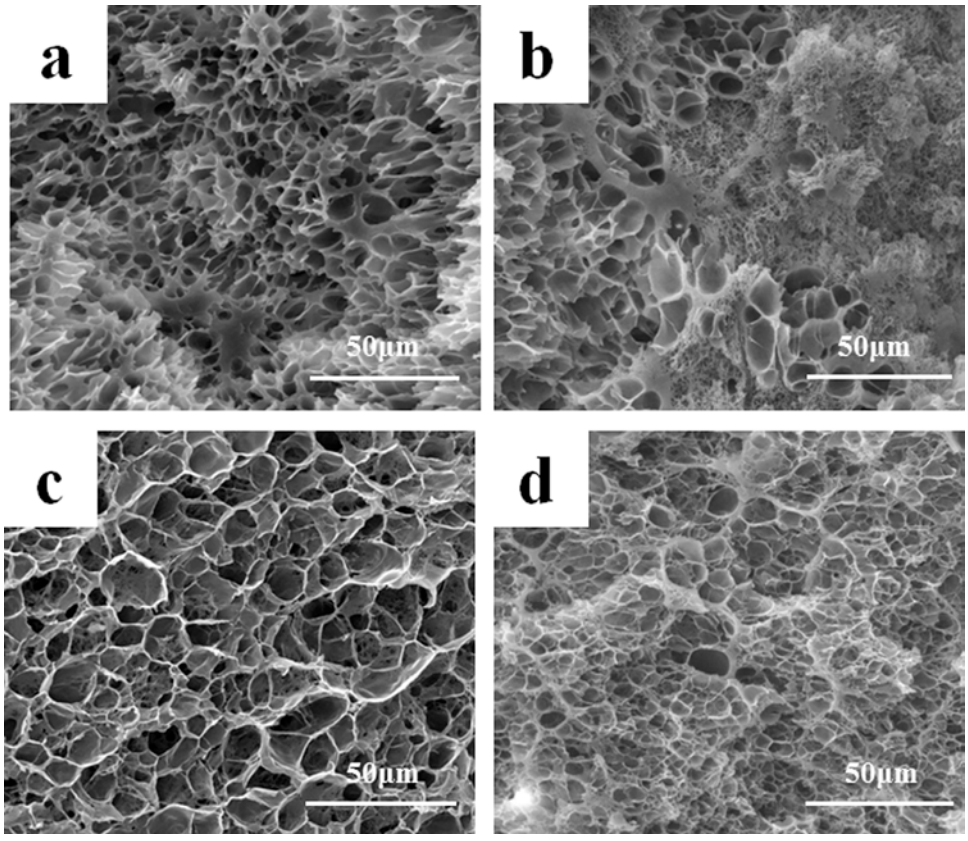

Fig. 9. SEM pictures of foamed iPP/0.2DMDBS, at a fixed foaming temperature of 165 °C, but different pressures of (a) 10 MPa, (b) 12 MPa, (c) 14 MPa, (d) 16 MPa.

Table 3
Average cell sizes, cell densities and foam densities of iPP/0.2DMDBS foamed at 165 °C, but different Pf, after a crystallization stage treatment.

P_f (MPa)	10	12	14	16
Cell size (μm)	7.11	1.13	9.41	4.00
Cell density (cells/cm^3)	8.27×10^{11}	1.17×10^{14}	5.55×10^{13}	8.40×10^{13}
Foam density (g/cm^3)	0.50	0.47	0.38	0.26

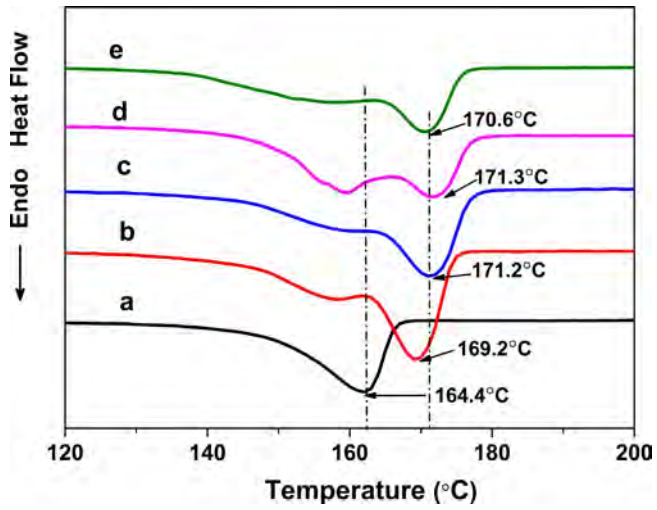

Fig. 10. DSC graphs of unfoamed pure iPP pellets (graph a), and foamed iPP/0.2DMDBS (graphs b–e) at a fixed foaming temperature of 165 °C, but different P_f of a at ambient pressure, b at 10 MPa, c at 12 MPa, d at 14 MPa, and e at 16 MPa.

the same as the foams in Fig. 9 applied. Fig. 11 shows the SEM pictures of foamed iPP/0.2DMDBS at different magnifications. In Fig. 11a,

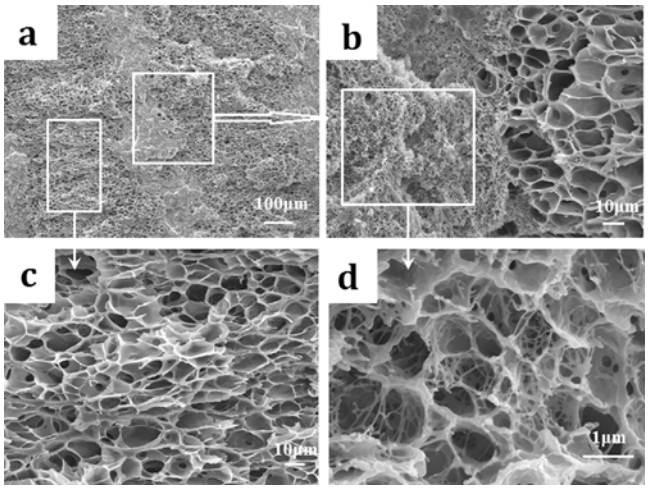

Fig. 11. SEM pictures of foamed iPP/0.2DMDBS, at T_f of 162 °C, P_f of 10 MPa, but different magnifications (a) ×100, (b), (c) ×800, (d) ×20, 000.

micron-sized (see Fig. 11c) and nano-sized (see Fig. 11d) cells alternately appear. The overall sample through the cross section reveals a sandwich structure distribution, due to the thermal varying and crystallization difference in these two locations. Average cell size of skin layer is about 380 nm to 6.11 μm, because of the fast crystallization and degassing of CO_2, this skin layer is a little bit solid than the inner layer next to it. To the core side, the average cell size is about 7.62 μm, the cell morphology is relatively uniform, as illustrated in Fig. 11c.

4. Conclusions

A step thermal control procedure was introduced in the batch foaming process of iPP and iPP/0.2DMDBS, rheological testing reveals

that the crystallization treatment could improve the storage modulus, loss modulus and complex viscosity in its semi-melting state (165 °C testing temperature), which means the improvement of elasticity and melt strength of iPP. Based on this strategy design, microcellular iPP foams in smaller size but higher cell density were fabricated through a suitable thermal control process. With the addition of DMDBS, the melt self-enhancement effect was magnified dramatically. The improvement of melt strength should be ascribed to the existence of partially structured melt, which was induced from former crystallization, partial melting, and annealing stages. Cooperated the step thermal treatment with the nucleating agent of 0.2 wt.% DMDBS, more uniform cells with much small sizes to nano-scaled and quite high cell densities up to 10^{14} cells/cm^3 were produced.

Acknowledgements

The authors thank the Microcellular Plastics Manufacturing Laboratory (MPML) of the University of Toronto, the National Natural Science Foundation of China (11372284), and the Henan Province Natural Science Projects of China (15A430049, 17A430005), for their financial supports.

Appendix A

1. SEM pictures of foamed iPP followed by a scheme as: Crystallized at a fixed P_a of 10 MPa, but different temperatures of T_a (a) 100 °C, (b) 110 °C, (c) 120 °C, (d) 130 °C, and T_f of 165 °C, P_f of 12 MPa.

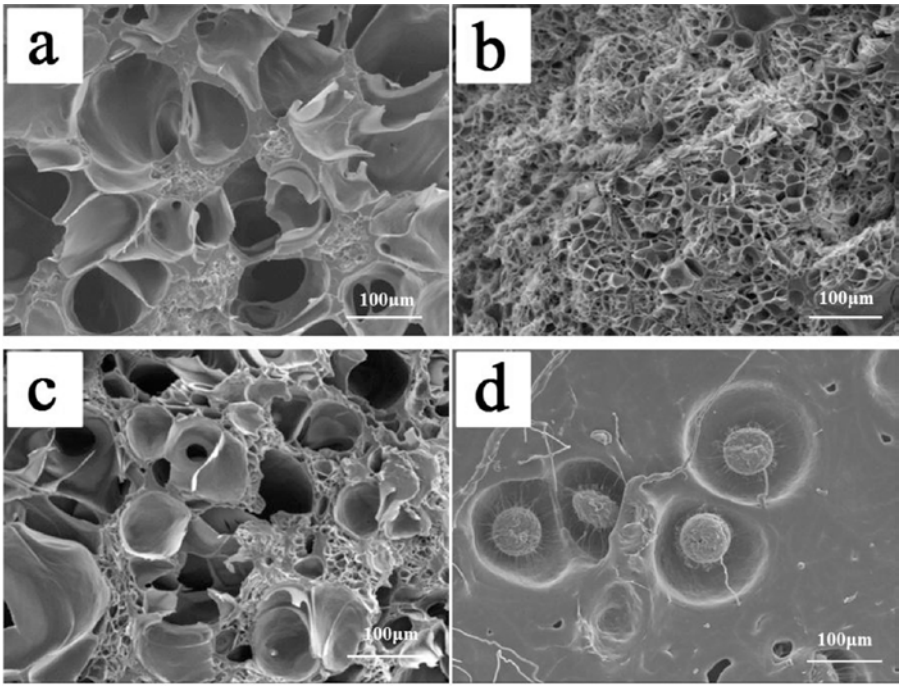

References

[1] J. Ding, J. Shangguan, W. Ma, Q. Zhong, Foaming behavior of microcellular foam polypropylene/modified nano calcium carbonate composites, J. Appl. Polym. Sci. 128 (2013) 3639–3651.
[2] J.W.S. Lee, C.B. Park, S.G. Kim, Reducing material costs with microcellular/fine-celled foaming, J. Cell. Plast. 43 (2016) 297–312.
[3] W. Zhai, Y.W. Kim, D.W. Jung, C.B. Park, Steam-chest molding of expanded polypropylene foams. 2. Mechanism of interbead bonding, Ind. Eng. Chem. Res. 50 (2011) 5523–5531.
[4] J.B. Bao, A. Nyantakyi Junior, G.S. Weng, J. Wang, Y.W. Fang, G.H. Hu, Tensile and impact properties of microcellular isotactic polypropylene (PP) foams obtained by supercritical carbon dioxide, J. Supercrit. Fluids 111 (2016) 63–73.
[5] S.H. Lee, M. Kontopoulou, C.B. Park, Effect of nanosilica on the co-continuous morphology of polypropylene/polyolefin elastomer blends, Polymer 51 (2010) 1147–1155.
[6] P.C. Lee, W. Kaewmesri, J. Wang, C.B. Park, J. Pumchusak, R. Folland, A. Praller, Effect of die geometry on foaming behaviors of high-melt-strength polypropylene with CO_2, J. Appl. Polym. Sci. 109 (2008) 3122–3132.
[7] W. Zhai, H. Wang, J. Yu, J.Y. Dong, J. He, Foaming behavior of isotactic polypropylene in supercritical CO_2 influenced by phase morphology via chain grafting, Polymer 49 (2008) 3146–3156.
[8] Y.G. Li, C.B. Park, Effects of branching on the pressure-volume-temperature behaviors, Ind. Eng. Res. 48 (2009) 6633–6640.
[9] W. Kaewmesri, P. Rachtanapun, J. Pumchusak, Effect of solvent plasticization on polypropylene microcellular foaming process and foam characteristics, J. Appl. Polym. Sci. 107 (2008) 63–70.
[10] Y. Li, Z. Yao, Z.H. Chen, S.L. Qiu, C. Zeng, K. Cao, High melt strength polypropylene by ionic modification: preparation, rheological properties and foaming behaviors, Polymer 70 (2015) 207–214.
[11] A. Rizvi, Z.K.M. Andalib, C.B. Park, Fiber-spun polypropylene/polyethylene terephthalate microfibrillar composites with enhanced tensile and rheological properties and foaming ability, Polymer 110 (2017) 139–148.
[12] H.X. Huang, H.F. Xu, Preparation of microcellular polypropylene/polystyrene blend foams with tunable cell structure, Polym. Adv. Technol. 22 (2011) 822–829.
[13] P. Rachtanapun, S.E.M. Selke, L.M. Matuana, Effect of the high-density polyethylene melt index on the microcellular foaming of high-density polyethylene/polypropylene blends, J. Appl. Polym. Sci. 93 (2004) 364–371.
[14] P. Rachtanapun, S.E.M. Selke, L.M. Matuana, Relationship between cell morphology and impact strength of microcellular foamed high-density polyethylene/polypropylene blends, Polym. Eng. Sci. 44 (2004) 1551–1560.
[15] P. Zhang, X.J. Wang, Y. Yang, N. Zhou, Effect of dynamic shear on the microcellular foaming of polypropylene/high-density polyethylene blends, J. Appl. Polym. Sci. 114 (2009) 1320–1328.
[16] W. Zhai, C.B. Park, Effect of nanoclay addition on the foaming behavior of linear polypropylene-based soft thermoplastic polyolefin foam blown in continuous extrusion, Polym. Eng. Sci. 51 (2011) 2387–2397.
[17] W.G. Zheng, Y.H. Lee, C.B. Park, Use of nanoparticles for improving the foaming behaviors of linear PP, J. Appl. Polym. Sci. 117 (2010) 2972–2979.
[18] H.X. Huang, J.K. Wang, Improving polypropylene microcellular foaming through blending and the addition of nano-calcium carbonate, J. Appl. Polym. Sci. 106 (2007) 505–513.
[19] J. Ding, W. Ma, F. Song, Q. Zhong, Effect of nano-calcium carbonate on microcellular foaming of polypropylene, J. Mater. Sci. 48 (2012) 2504–2511.
[20] R. Miyamoto, S. Yasuhara, H. Shikuma, M. Ohshima, Preparation of micro/

nanocellular polypropylene foam with crystal nucleating agents, Polym. Eng. Sci. 54 (2014) 2075–2085.
[21] P. Rachtanapun, S.E.M. Selke, L.M. Matuana, Microcellular foam of polymer blends of HDPE_PP and their composites with wood fiber, J. Appl. Polym. Sci. 88 (2003) 2842–2850.
[22] A.K. Bledzki, O. Faruk, Injection moulded microcellular wood fibre-polypropylene composites, Composites Part A: Appl. Sci. Manuf. 37 (2006) 1358–1367.
[23] F.A. Soares, S.M.B. Nachtigall, Effect of chemical and physical foaming additives on the properties of PP/wood flour composites, Polym. Test. 32 (2013) 640–646.
[24] Z.X. Zhang, D.L. Chen, K.H. Kwak, Z.X. Xin, J. Kuk Kim, Effects of compatibilizers on the physico-mechanical and foaming properties of polyproylene/wood-fiber composites, J. Vinyl Add. Technol. 19 (2013) 250–257.
[25] X. Liao, A.V. Nawaby, P.S. Whitfield, Carbon dioxide-induced crystallization in poly (L-lactic acid) and its effect on foam morphologies, Polym. Int. 59 (2010) 1709–1718.
[26] X.L. Jiang, T. Liu, Z.M. Xu, L. Zhao, G.H. Hu, W.K. Yuan, Effects of crystal structure on the foaming of isotactic polypropylene using supercritical carbon dioxide as a foaming agent, J. Supercrit. Fluids 48 (2009) 167–175.
[27] D.C. Li, T. Liu, L. Zhao, W.K. Yuan, Foaming of linear isotactic polypropylene based on its non-isothermal crystallization behaviors under compressed CO_2, J. Supercrit. Fluids 60 (2011) 89–97.
[28] Y.G. Li, C.B. Park, H.B. Li, J. Wang, Measurement of the PVT property of PP/CO2 solution, Fluid Phase Equilib. 270 (2008) 15–22.
[29] Z.M. Xu, X.L. Jiang, T. Liu, G.H. Hu, L. Zhao, Z.N. Zhu, W.K. Yuan, Foaming of polypropylene with supercritical carbon dioxide, J. Supercrit. Fluids 41 (2007) 299–310.
[30] X. Sun, H. Kharbas, J. Peng, L.S. Turng, A novel method of producing lightweight microcellular injection molded parts with improved ductility and toughness, Polymer 56 (2015) 102–110.
[31] J.I. Velasco, M. Antunes, V. Realinho, M. Ardanuy, Characterization of rigid polypropylene-based microcellular foams produced by batch foaming processes, Polym. Eng. Sci. 51 (2011) 2120–2128.
[32] M. Antunes, V. Realinho, J.I. Velasco, Study of the influence of the pressure drop rate on the foaming behavior and dynamic-mechanical properties of CO2 dissolution microcellular polypropylene foams, J. Cell. Plast. 46 (2010) 551–571.
[33] S. Doroudiani, C.B. Park, M.T. Kortschot, Effect of the crystallinity and morphology on the microcellular foam structure of semicrystalline polymers, Polym. Eng. Sci. 36 (1996) 2645–2662.
[34] D.F. Baldwin, C.B. Park, N.P. Suh, A microcellular processing study of poly(ethylene terephthalate) in amorphous and semicrystalline states. Part I: microcell nucleation, Polym. Eng. Sci. 36 (1996) 1437–1445.
[35] D.F. Baldwin, C.B. Park, N.P. Suh, A microcellular processing study of poly(ethylene terephthalate) in amorphous and semicrystalline states. Part II: cell growth and process design, Polym. Eng. Sci. 36 (1996) 1446–1453.
[36] S. Doroudiani, C.B. Park, M.T. Kortschot, Effect of the crystallinity and morphology on the microcellular foam structure of semicrystalline polymers, Polym. Eng. Sci. 36 (1996) 2645–2662.
[37] W.T. Zhai, Y. Ko, W.L. Zhu, A. Wong, C.B. Park, A study of the crystallization, melting, and foaming behaviors of polylactic acid in compressed CO_2, Int. J. Mol. Sci. 10 (2009) 5381–5397.
[38] X.Y. Zhu, Y.J. Li, D.Y. Yan, Crystallization behavior of partially melting isotactic polypropylene, Polymer 22 (2001) 9217–9222.
[39] B. Zhang, J. Chen, F. Ji, X. Zhang, G. Zheng, C. Shen, Effects of melt structure on shear-induced β-cylindrites of isotactic polypropylene, Polymer 53 (2012) 1791–1800.
[40] B. Zhang, J. Chen, X. Zhang, C. Shen, Crystal morphology and structure of the β-form of isotactic polypropylene under supercooled extrusion, J. Appl. Polym. Sci. 120 (2011) 3255–3264.
[41] B. Zhang, J. Chen, X. Zhang, C. Shen, Formation of β-cylindrites under supercooled extrusion of isotactic polypropylene at low shear stress, Polymer 52 (2011) 2075–2084.
[42] C. Zhang, H. Hu, D. Wang, S. Yan, C.C. Han, In situ optical microscope study of the shear-induced crystallization of isotactic polypropylene, Polymer 46 (2005) 8157–8161.
[43] A. Ameli, D. Jahani, M. Nofar, P.U. Jung, C.B. Park, Processing and characterization of solid and foamed injection-molded polylactide with talc, J. Cell. Plast. 49 (2013) 351–374.
[44] Y. Wang, J.Z. Xu, Y.H. Chen, K. Qiao, L. Xu, X. Ji, Z.M. Li, B.S. Hsiao, Crystalline structure changes in preoriented metallocene-based isotactic polypropylene upon annealing, J. Phys. Chem. B 117 (2013) 7113–7122.
[45] Y. Gao, X. Dong, L. Wang, G. Liu, X. Liu, C. Tuinea-Bobe, B. Whiteside, P. Coates, D. Wang, C.C. Han, Flow-induced crystallization of long chain aliphatic polyamides under a complex flow field: inverted anisotropic structure and formation mechanism, Polymer 73 (2015) 91–101.
[46] D. Raps, T. Köppl, A.R. de Anda, V. Altstädt, Rheological and crystallisation behaviour of high melt strength polypropylene under gas-loading, Polymer 55 (2014) 1537–1545.
[47] T.J. McCallum, M. Kontopoulou, C.B. Park, E.B. Muliawan, S.G. Hatzikiriakos, The rheological and physical properties of linear and branched polypropylene blends, Polym. Eng. Sci. 47 (2007) 1133–1140.
[48] S. Tan, A. Su, J. Luo, E. Zhou, Crystallization kinetics of poly ether ether ketone PEEK from its metastable melt, Polymer 40 (1999) 1223–1231.
[49] J. Zhang, K. Tashiro, H. Tsuji, A. Domb, Disorder-to-order phase transition and multiple melting behavior of poly (L-lactide) investigated by simutaneous measurements of WAD and DSC, Macromolecules 41 (2008) 1352–1357.
[50] G.F. Shan, W. Yang, X.G. Tang, M.B. Yang, B.H. Xie, Q. Fu, Y.W. Mai, Multiple melting behaviour of annealed crystalline polymers, Polym. Test. 29 (2010) 273–280.
[51] K.C. Mai, K.F. Wang, H.M. Zeng, Multiple melting behavior of nucleated polypropylene, J. Appl. Polym. Sci. 88 (2003) 1608–1611.
[52] Z. Zhang, A.V. Nawaby, M. Day, CO_2-delayed crystallization of isotactic polypropylene: a kinetic study, J. Polym. Sci. Polym. Phys. 41 (2003) 1518–1525.
[53] N. Patil, C. Invigorito, M. Gahleitner, S. Rastogi, Influence of a particulate nucleating agent on the quiescent and flow-induced crystallization of isotactic polypropylene, Polymer 54 (2013) 5883–5891.